International Journal of Engineering

An Efficient Curvelet Framework for Denoising Images

E. Ehsaeyan

Department of Electrical and Electronics Engineering, Sirjan University of Technology

P A P E R   I N F O

A B S T R A C T

Wiener filter suppresses noise efficiently. However, it makes the output image blurred. Curvelet preserves the edges of natural images perfectly, but, it produces visual distortion artifacts and fuzzy edges to the restored image, especially in homogeneous regions of images. In this paper, an efficient image denoising framework based on Curvelet transform and wiener filter is proposed, which can reduce noise better than these methods. The performance of introduced scheme is evaluated in terms of two important denoising criteria, PSNR and SSIM on standard test images in different noise levels. Three famous thresholding 'soft', 'semisoft' and 'hard' are applied to noisy images and results are fused by the wavelet transform to form restore images. Our framework outperforms the curvelet transform denoising by %6.3 in terms of PSNR and %5.9 in terms of SSIM for 'Lena' image. The visual outputs show that false artifacts, parasite lines and the blurring degree of output images, are reduced significantly. The obtained results reveal the superiority of our framework over recent reported methods.

doi: 10.5829/idosi.ije.2016.29.08b.09

1. INTRODUCTION

The image enhancement and image restoration are the essential processes in practical applications [1-5]. The main goal of denoising is to suppress noise from observed images and present a refined image with high similarity to the original image. Wavelet transform is a powerful tool to present the singularity of images. However, it cannot represent smooth edges properly.

Curvelet transform as a multiresolution geometric analysis is introduced by Donoho and Candes [6-8]. Stehly et al. have utilized curvelet transform in computing synthetic noise correlation to improve ambient noise tomography [9]. A Poisson noise removal algorithm based on fast curvelet transform and multiscale variance stabilizing transform and wave atom has been reported [10]. In another research, curvelet transform and total variation methods have been used in denoising CT and MRI images [11].

A Wiener filtering algorithm with pseudo-inverse technique solving the Gaussian noise problem for

ultrasound image by setup a constant dB of noise function has been introduced [12]. A denoising method based on nonlocal neutro-sophic set (NLNS) approach of Wiener filtering has been proposed and the results have been compared with similar methods such as classical Wienerfilter, the anisotropic diffusion filter, the total variation minimization and the nonlocal means filter [13]. In another paper, a gradient-based Wiener filter (GWF) for image denoising has been suggested [14]. This filter is implemented by a local adaptive denoising algorithm based on the Wiener-like shrinkage function in the gradient domain.

In this paper, an efficient denoising framework, which consists of the curvelet transform and Wiener filter stages, is proposed. Wiener filter minimizes mean square error (MSE) and blocks noise efficiently. However, it yields an artificial denoised image, which has poor similarity to the original image. It means that the output has a cartoon-like appearance. Furthermore, it makes output images blurred. On the other side, curvelet transform does not vanish the image. However, it is an orientated transform and produces false curved lines, which are observable in the restored image. We combine these two methods with different properties

 Corresponding Author's Email: ehsaeyan@sirjantech.ac.ir (E. Ehsaeyan)

and utilize a wavelet-based fusion method to introduce an efficient framework with better performance. It will be shown that the denoised images would be less blurred with vanished line artifacts.

The rest of this paper is organized as follows: section 2 describes the proposed framework in four stages: Wiener filter, curvelet transform, thresholding and the fusion method. In each part, the subject with relevant formulas is explained briefly. Section 3 presents the results obtained in terms of PSNR and SSIM. Visual results are given to compare our method with the Wiener filter and curvelet transform. A discussion on fusion methods and efficiency of the curvelet and wavelet methods is presented in this section. Finally, a conclusion of the paper is given in section 4.

2. PROPOSED FRAMEWORK

Figure 1 shows the block diagram of the proposed scheme. The proposed denoising procedure consists of three main parts which are described as follows: at first, by applying Wiener filter to the input image, the noised is suppressed and diluted. However, it is not sufficient because, the output would be a blurred and cartoon-like image. For quality enhancement, the difference between the input image and the output of Wiener filter is applied to the curvelet transform stage. This difference has details and it is important to refine because noise corrupts the details more than approximation. So, the duty of the curvelet transform is to distinguish fake and real details in directional bands.To make this decision, three thresholding methods i.e. 'soft', 'semisoft' and 'hard' are applied to subband coefficients in thresholding block. Then, an inverse curvelet transform is used to obtain refined details. This noiseless detail is added to the output of wiener filter to compensate the quality of the details.Finally, as shown in Figure 1, the two denoised images are applied to the fusion stage. This block combines two inputs and yields a restored image which has less blurring properties and artifact lines.In the following, we discuss these four blocks in detail.
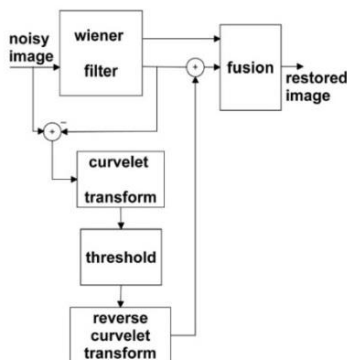

Figure 1. Proposed denoising method block diagram

2. 1. Wiener Filter Stage   In image denoising, the Wiener filter is a filter used to produce an estimate of a desired or target random process by linear time-invariant (LTI) filtering of a noisy input image, assuming known stationary signal, noise spectra, and additive noise. The Wiener filter minimizes the mean square error between the observed image and original image.

The main purpose of the Wiener filter is to determine a statistical estimate of an unknown signal using a related image as an input and filtering that known image to produce the estimate as an output. For example, the known image might consist of an unknown image of interest that has been corrupted by additive noise. The Wiener filter can be used to filter out the noise from the corrupted image to provide an estimate of the underlying original image. It is based on a statistical theory, and a more statistical account of the theory is given in the minimum mean-square error (MMSE) article.

The Wiener filtering is optimal in terms of the mean square error, where the noise is AWGN. It means that it minimizes the MSE in the process of inverse filtering and noise smoothening. The Wiener filtering is a linear estimation of the original image. The approach is based on a stochastic framework. The Wiener filter in Fourier transform domain can be calculated as [15]:

$$W(u,v) = \frac{1}{H(u,v)} \frac{|H(u,v)|^2}{|H(u,v)|^2 + S_\eta(u,v)/S_f(u,v)} \qquad (1)$$

Where, $H(u,v)$ is the degradation function of noise, $S_\eta(u,v)$ and $S_f(u,v)$ are the power spectrum of the noise and the power spectrum of the original image, respectively. In this paper, we use an adaptive Wiener filter. This filter estimates the local mean and variance around each pixel as:

$$\mu = \frac{1}{MN} \sum_{n_1,n_2 \in \eta} I(n_1,n_2) \qquad (2\text{-}a)$$

$$\sigma^2 = \frac{1}{MN} \sum_{n_1,n_2 \in \eta} I^2(n_1,n_2) - \mu^2 \qquad (2\text{-}b)$$

Where, η is the N-by-M local neighborhood of each pixel in the image I. Adaptive Wiener filter uses these pixel wise estimates [16]:

$$b(n_1,n_2) = \mu + \frac{\sigma^2 - v^2}{\sigma^2}(I(n_1,n_2) - \mu) \qquad (3)$$

Where, v^2 is the noise variance.

2. 2. Curvelet Transform Stage   Curvelets are non-adaptive methods for multi-direction object representation. Being an extension of the wavelet concept, they are becoming popular in similar fields, namely in image denoising and image retrieval.

Wavelets accomplished the Fourier transform by using a basis that represents both location and spatial frequency. For images, directional wavelet transforms go further, by using basis functions that are also localized in orientation (like Dual-Tree Complex Wavelet Transform).

A curvelet transform has different properties compared to other directional wavelet transforms in that the amount of localization in orientation varies with scale. Specially, fine-scale basis functions are long ridges; the shape of the basis functions at scale j is 2^{-j} by $2^{-j/2}$, therefore the fine-scale bases are skinny ridges with a precisely determined direction.

Curvelets are appropriate tools for representing images (or other functions) which are smooth apart from singularities along smooth curves, where the curves have bounded curvature, i.e. where objects in the image have a minimum length scale. This property holds for cartoons, geometrical diagrams, and text. As one zooms in on such images, the edges and corners they contain appear increasingly straight. Curvelets take advantage of this property, by defining the higher resolution curvelets to be more elongated than the lower resolution curvelets. However, natural images do not have this property; they have details at every scale. Therefore, for these images, it is better to use some sort of directional wavelet transform whose wavelets have the same aspect ratio at every scale. A curvelet transform is determined under the following steps [17]:

Subband decomposition: With *a_terous* algorithm, the image passes through lowpass filter P_0 and bandpass Δs:

$$f \rightarrow (P_0 f, \Delta_1 f, \Delta_2 f, \dots) \tag{4}$$

Smoothing: Each band is smoothed and windowed as:

$$h_Q = W_Q . \Delta_s f \ , \ \forall Q \in Q_s \tag{5}$$

where W_Q is window function and Q is dyadic function which is defined at scale s as:

$$Q(s, k_1, k_2) = \left[\frac{k_1}{2^s}, \frac{k_1+1}{2^s}\right] * \left[\frac{k_2}{2^s}, \frac{k_2+1}{2^s}\right] \tag{6}$$

where k_1 and k_2 indicate length of the filter.

Normalization: Every window is renormalized in the range [0,1] by:

$$g_Q = T_Q^{-1} . h_Q \tag{7}$$

Where, T_Q is the normalizer function.

Ridgelet analysis: Ridgelet of a 2D function is defined as:

$$R_f(a, b, \theta) = \int f(x_1, x_2) \Psi_{(a,b,\theta)}(x_1, x_2) dx_1 dx_2 \tag{8-a}$$

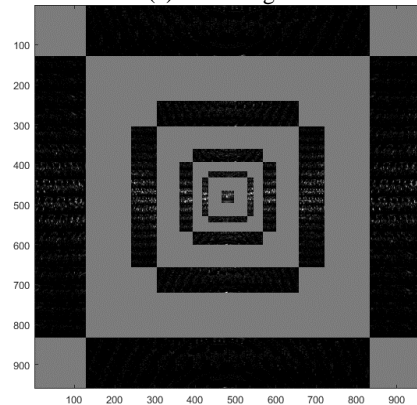$$\Psi_{(a,b,\theta)}(x) = a^{1/2} \Psi \left(\frac{x_1 cos\theta + x_2 sin\theta - b}{a}\right) \tag{8-b}$$

where, a, b and θ are the scale, location and orientation parameters, respectively, and Ψ is the wavelet function. Figure 2 displays the curvelet transform of a test image.

2. 3. Thresholding   Hard, soft and semisoft thresholding are three main thresholding methods, which are defined as [18, 19]:

$$S_T^{hard}(x) = \begin{cases} x & if \ |x| > T \\ 0 & if \ |x| \le T \end{cases} \tag{9-a}$$

(a) Test image

(b) Curvelet coefficients

Figure 2. Test image and curvelet coefficients. In this image, the low frequency (coarse scale) coefficients are stored at the center of the display. The Cartesian concentric coronae shows the coefficients at different scales; the outer coronae correspond to higher frequencies. There are four strips associated to each corona, corresponding to the four cardinal points; these are further subdivided in angular panels. Each panel represents coefficients at a specified scale and along the orientation suggested by the position of the panel.

$$S_T^{soft}(x) = \max\left(1 - \frac{T}{|x|}\right) x \tag{9-b}$$

$$S_T^{semisoft}(x) = \begin{cases} 0 & |x| \le T_1 \\ x & |x| > T_2 \\ sgn(x) \times \frac{T_2|x|-T_1}{T_2-T_1} otherwise \end{cases} \tag{9-c}$$

Hard and soft thresholding are two specific non-linear diagonal estimators, but one can optimize the non-linearity to capture the distribution of wavelet coefficient of a class of images. Semi-soft thresholding is a family of non-linearities that interpolates between soft and hard thresholding. It uses both a main threshold T_1 and a secondary threshold $T_2 = \mu T_1$. When $\mu = 1$, the semi-soft thresholding performs a hard thresholding, whereas when $\mu = \infty$, it performs a soft thresholding.

'Block' thresholding is another method, which applies the thresholding rule on a group of coefficients instead of a single coefficient. Each band is divided to

disjoint blocks and all coefficients within a block, are attenuated with a same factor [20].

2. 4. Fusion Stage   Image fusion is the process of combining relevant information from two or more images into a single image [21]. The resulting image will be more informative than any of the input images [22]. Image fusion methods can be broadly classified in two groups, spatial domain fusion and transform domain fusion.

In this paper, a wavelet-based transform fusion is used. Image fusion by wavelet transform is a common way to combine two images [23]. Figure 3 indicates the procedure. By applying wavelet transform, two images are decomposed to approximation and detail coefficients. The fusion rule is as follows: an average of approximation coefficients is taken, and the minimum of detail coefficient belongs to each band is selected to form a new decomposition. Finally, with applying inverse wavelet transform, the denoised image is achieved. In the next section, we will discuss the reason to use this structure.

3. RESULTS AND DISCUSSIONS

In this section, we present results in various noise conditions to evaluate the efficiency of the proposed scheme. First, we review important image denoising criteria.Three quality criteria are considered in this paper. Peak Signal to Noise Ratio (PSNR) as a well-known survey is used to calculate errors between original and restored images. The second one is Structural Similarity or SSIM.
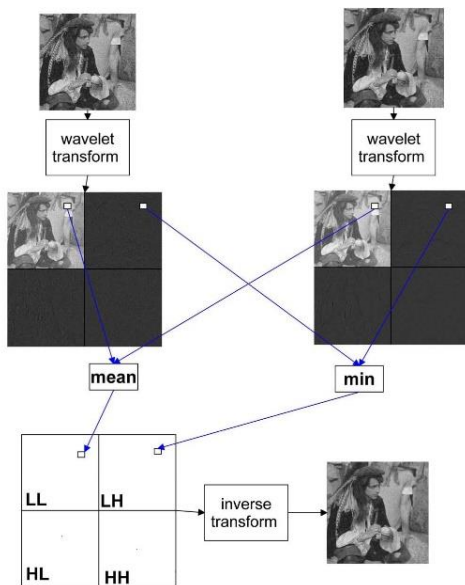

Figure 3. Wavelet-based fusion structure

The Structural Similarity (SSIM) Index quality assessment index is based on the computation of three terms, namely the luminance term, the contrast term and the structural term. The overall index is a multiplicative combination of the three terms [24]:

$$SSIM(x,y) = [I(x,y)]^{\alpha}.[c(x,y)]^{\beta}[s(x,y)]^{\gamma} \qquad (10)$$

where:

$$I(x,y) = \frac{2\mu_x\mu_y + c_1}{\mu_x^2 + \mu_y^2 + c_1} \qquad (11\text{-a})$$

$$c(x,y) = \frac{2\sigma_x\sigma_y + c_2}{\sigma_x^2 + \sigma_y^2 + c_2} \qquad (11\text{-b})$$

$$s(x,y) = \frac{\sigma_{xy} + c_3}{\sigma_x\sigma_y + c_3} \qquad (11\text{-c})$$

where μ_x, μ_y, σ_x,σ_y, and σ_{xy} are the local means, standard deviations, and cross-covariance for images x, y and c_1,c_2,c_3 are constant parameters. In order to simplify SSIM expression, $\alpha = \beta = \gamma = 1$and $c_3 = \frac{c_2}{2}$ are assumed like ref [24].

Third criterion is Universal Index [25]. Universal Index is designed by modeling any image distortion as a combination of three factors: loss of correlation, luminance distortion, and contrast distortion.

The proposed method is compared to state-of-the-art methods to assess the denoising effectiveness. Namely, SURELET [26], Bivariate [27], Bayes [28], LLSURE [29], guided image filter (GIF) [30], fast bilateral filter (FBF) [31] and total variation (TV) [32]. Images are corrupted by Additive White Gaussian Noise (AWGN) with different noise levels from 10 to 35. PSNR (in dB), SSIM and FOM [33] values of the denoised images relative to their original images using such methods are reported in Tables 1, 2 and 3, respectively. In a general overview, our scheme has better results compared to state-of-art methods.

In Figure 4, Wiener denoising, curvelet denoising and proposed method are compared by Universal Index for 'man' image.

The obtained results confirm that the proposed algorithm gives highest Universal Index compared to other methods.

Figure 5 shows comparative results for denoising image 'Man' in the visual mode. If we focus on details, we will find out the wiener filter makes images blurred, and the result seems artificial.

In turn, curvelet transform does not blur images. However, it adds some line-shape artifacts to the denoised image. Our framework has a better act in denoising. Because, the results are not so blurred and line-shape artifacts are suppressed efficiently.

The proposed approach can reduce the blurriness imposed by the Wiener filter. A blur metric which has been introduced in [34], is used to evaluate the blur introduced by a restoration processing. Results are shown in Table 4.

TABLE 1. PSNRs (in dB) of restored imagesofwell-known methods

image	sigma	Wiener filter	LLSURE method	GIF method	FBF method	TV method	SURELET method	Bivariate method	Bayes method	Proposed method
Lena	10	30.46	31.33	30.56	30.53	30.47	30.94	30.02	29.97	34.11
	15	29.52	29.09	28.23	28.21	28.40	28.50	27.12	27.30	32.62
	20	28.63	27.76	26.56	26.12	26.92	26.99	25.14	25.96	31.21
	25	27.84	26.38	25.52	24.14	25.84	26.07	23.84	23.75	30.29
	30	27.14	25.37	24.35	23.12	24.94	25.04	23.10	23.09	29.44
	35	26.52	24.45	23.89	22.78	24.34	24.42	22.20	22.51	28.48
Barbara	10	27.49	30.57	30.03	29.81	29.89	30.30	29.24	29.56	32.08
	15	26.79	28.20	27.32	27.10	27.68	26.84	26.43	27.12	31.26
	20	26.09	26.65	25.78	25.86	26.26	26.19	24.40	24.93	30.08
	25	25.45	25.64	24.13	24.88	25.25	25.25	23.26	23.96	29.55
	30	24.89	24.83	23.09	23.98	24.36	24.24	22.02	22.52	28.82
	35	24.39	23.39	22.36	23.14	23.58	23.58	21.42	22.14	26.17
Boat	10	28.50	30.88	30.03	29.95	29.64	30.68	29.96	29.76	30.85
	15	27.78	28.60	27.62	27.69	27.43	28.07	27.12	27.16	29.79
	20	27.06	26.87	25.42	25.48	26.02	26.51	25.00	24.99	28.85
	25	26.40	25.76	24.32	24.49	24.97	25.34	23.90	24.07	28.03
	30	25.80	24.48	23.29	23.51	24.19	24.61	22.53	23.07	27.31
	35	25.27	23.81	22.59	22.87	23.55	23.95	21.85	21.95	26.65
Peppers	10	28.73	30.91	30.36	30.37	29.94	30.53	29.62	29.58	33.43
	15	27.95	28.60	27.71	27.72	27.61	28.01	26.63	27.04	32.17
	20	27.14	27.35	26.07	26.15	26.08	26.58	24.70	24.96	31.07
	25	26.37	25.86	24.48	24.73	24.87	25.24	23.27	23.99	30.08
	30	25.67	24.74	23.65	23.86	23.86	24.50	22.41	22.57	29.36
	35	25.05	23.97	22.76	22.89	23.07	23.86	21.13	21.59	28.39

TABLE 2. SSIM values for standard images with different noise power

image	sigma	Wiener filter	LLSURE method	GIF method	FBF method	TV method	SURELET method	Bivariate method	Bayes method	Proposed method
Lena	10	0.77	0.92	0.91	0.91	0.91	0.90	0.85	0.88	0.90
	15	0.74	0.89	0.89	0.87	0.87	0.85	0.76	0.82	0.87
	20	0.72	0.85	0.83	0.84	0.83	0.80	0.67	0.77	0.85
	25	0.70	0.81	0.80	0.79	0.80	0.76	0.60	0.65	0.82
	30	0.68	0.78	0.76	0.74	0.77	0.72	0.54	0.62	0.78
	35	0.66	0.75	0.74	0.71	0.74	0.68	0.48	0.56	0.75
Barbara	10	0.76	0.92	0.90	0.91	0.91	0.91	0.87	0.89	0.90
	15	0.74	0.88	0.87	0.89	0.86	0.85	0.77	0.83	0.86
	20	0.71	0.83	0.81	0.81	0.82	0.80	0.69	0.75	0.80
	25	0.68	0.80	0.80	0.79	0.78	0.76	0.62	0.71	0.76
	30	0.66	0.77	0.78	0.77	0.74	0.73	0.55	0.62	0.74
	35	0.63	0.74	0.71	0.72	0.71	0.69	0.49	0.60	0.70
Boat	10	0.70	0.92	0.91	0.92	0.90	0.90	0.85	0.87	0.80
	15	0.67	0.87	0.88	0.89	0.85	0.85	0.75	0.80	0.77
	20	0.65	0.83	0.82	0.81	0.81	0.79	0.66	0.68	0.74
	25	0.63	0.79	0.81	0.79	0.77	0.74	0.58	0.66	0.71
	30	0.61	0.74	0.72	0.70	0.73	0.70	0.52	0.62	0.68
	35	0.59	0.71	0.69	0.69	0.70	0.66	0.47	0.52	0.66
Peppers	10	0.81	0.93	0.91	0.90	0.93	0.91	0.86	0.88	0.85
	15	0.79	0.90	0.88	0.89	0.89	0.86	0.77	0.82	0.82
	20	0.76	0.87	0.86	0.83	0.86	0.82	0.68	0.75	0.79
	25	0.73	0.84	0.82	0.81	0.83	0.78	0.62	0.72	0.77
	30	0.71	0.81	0.79	0.78	0.80	0.74	0.56	0.63	0.74
	35	0.69	0.79	0.76	0.74	0.77	0.71	0.51	0.58	0.72

TABLE 3. FOM values for standard images with different noise power

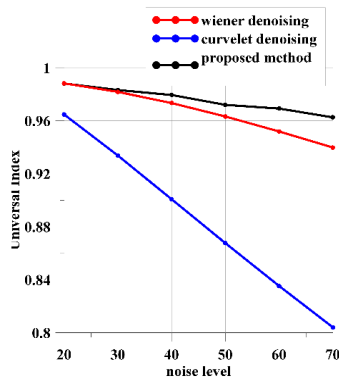| image	sigma	Wiener filter	LLSURE method	GIF method	FBF method	TV method	SURELET method	Bivariate method	Bayes method	Proposed method
Lena	10	0.86	0.92	0.92	0.91	0.90	0.94	0.96	0.94	0.97
	15	0.84	0.90	0.90	0.89	0.88	0.92	0.95	0.93	0.95
	20	0.79	0.86	0.85	0.86	0.83	0.91	0.93	0.93	0.9
	25	0.77	0.84	0.84	0.83	0.81	0.89	0.90	0.90	0.88
	30	0.76	0.84	0.82	0.83	0.80	0.88	0.88	0.88	0.87
	35	0.72	0.82	0.82	0.81	0.76	0.88	0.83	0.88	0.83
Barbara	10	0.85	0.92	0.93	0.92	0.89	0.93	0.96	0.95	0.96
	15	0.80	0.89	0.90	0.90	0.84	0.92	0.94	0.94	0.91
	20	0.77	0.82	0.86	0.85	0.81	0.90	0.92	0.92	0.88
	25	0.74	0.82	0.85	0.83	0.78	0.89	0.90	0.90	0.85
	30	0.71	0.80	0.81	0.81	0.75	0.87	0.88	0.88	0.82
	35	0.68	0.76	0.77	0.80	0.72	0.86	0.86	0.87	0.79
Boat	10	0.88	0.95	0.93	0.92	0.92	0.95	0.94	0.96	0.97
	15	0.86	0.92	0.91	0.91	0.90	0.94	0.92	0.93	0.95
	20	0.80	0.90	0.90	0.91	0.84	0.92	0.88	0.90	0.91
	25	0.79	0.85	0.86	0.87	0.83	0.87	0.85	0.85	0.9
	30	0.71	0.83	0.84	0.82	0.75	0.85	0.81	0.82	0.82
	35	0.71	0.80	0.79	0.80	0.75	0.82	0.75	0.79	0.82
Peppers	10	0.89	0.94	0.94	0.92	0.93	0.96	0.96	0.96	0.97
	15	0.84	0.90	0.89	0.89	0.88	0.93	0.95	0.94	0.95
	20	0.80	0.85	0.84	0.86	0.84	0.92	0.92	0.93	0.91
	25	0.77	0.84	0.83	0.84	0.81	0.89	0.91	0.91	0.88
	30	0.74	0.81	0.80	0.80	0.78	0.87	0.89	0.90	0.85
	35	0.72	0.80	0.78	0.79	0.76	0.89	0.87	0.88	0.83

Figure 4. Universal Index results of three denoising methods: Wiener filter, curvelet transform and ours. The results have been calculated for 'man' image.
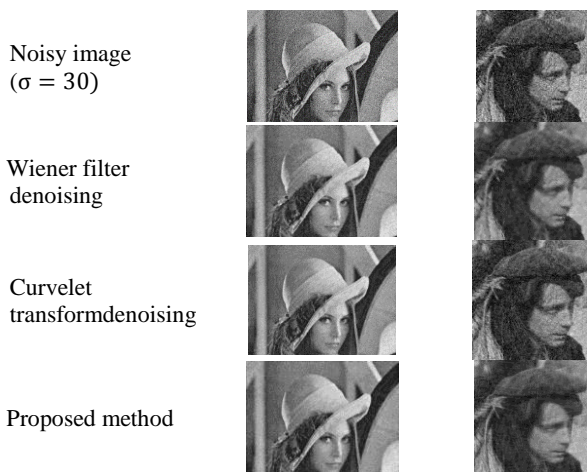

Figure 5. Visual comparative denoising results for images 'Lena' and 'Man'

TABLE 4. Perceptual blur metric of different images in noise level 20 (the output is in [0,1]; 0 means sharp, 1 means blur)

image	Original image	Recovered by Wiener filter	Recovered by proposed method
Lena	0.3666	0.4618	0.4363
Barbara	0.2367	0.3902	0.3763
Boat	0.2949	0.424	0.4108
Peppers	0.3609	0.5136	0.4582

It is clear that our method preserves details better than the Wiener filter. Furthermore, our method has been implemented with Discrete Wavelet Transform (DWT) and Double Density Wavelet Transform (DDWT) instead of curvelet transform.

The double-density DWT is an improvement upon the critically sampled DWT with important additional following properties: (1) It employs one scaling function and two distinct wavelets, which are designed to be offset from one another by one half, (2) The double-density DWT is overcomplete by a factor of two, and (3) It is nearly shift-invariant. Figure 6 shows PSNR for 'Goldhill' image with applying the 'block' thresholding method. From given curves, it is obvious that curvelet transform has higher PSNR between all.

As was mentioned in Section 2, two groups of fusion are used in the introduced scheme: spatial and transform fusion. A wavelet based structure as shown in Figure 3, has been selected in this paper. Three fusion methods have been implemented and examined in our framework: average, wavelet and Pulse Coupled Neural

Networks (PCNN) [35]. Results have been shown in Figure 7 for 'barbara' image with the 'blocking' threshold method. Average is the simplest way to fuse two images, which has low computational cost. The output is moderate in every noise condition. PCNN method acts according to focus objects. However, it is a high computational and noise sensitive method. Wavelet method has a better performance in the high noise polluted case with lower execution time compared to PCNN method.

Among wavelet fusion methods, mean-min (average coefficients in lowpass band – minimum coefficients in highpass bands) has been selected due to better performance. Figure 8 shows the effects of different rules on PSNR of fusion 'Barbara' image versus noise levels.

Figure 9 shows four original and corresponding noisy images as well as denoised images obtained through the application of other denoising methods being compared. Bayes wavelet-based methods tend to produce smoothed results in homogeneous regions. Nevertheless, certain features such as edges are affected.

Table 5 compares proposed framework with other recent reported works. The highest PSNR is bolded in the specified noise level. From given data, it is clear that our method has a better performance to stop noise in most cases.
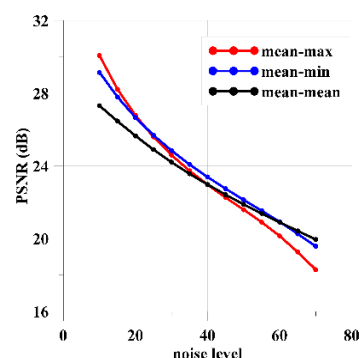

Figure 8. PSNR results of three wavelet fusion methods: average, minimum and maximum. The results have been calculated for image 'Barbara' with 'block' thresholding rule.
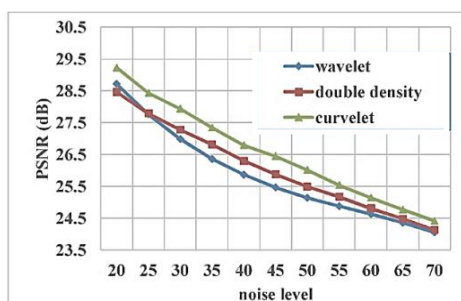

Figure 6. Implementing proposed framework with wavelet, double density wavelet and curvelet transform
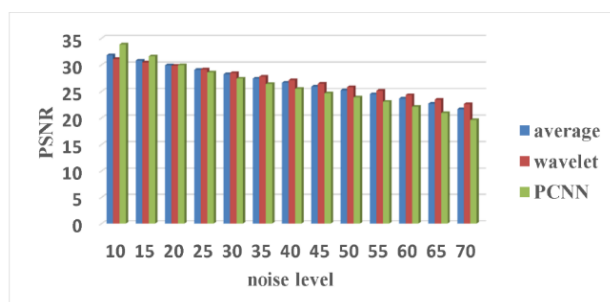

Figure 7. PSNR results of three fusion methods: average, discrete wavelet transform (DWT) and Pulse Coupled Neural Networks (PCNN). The results have been calculated for image 'Barbara' with 'block' thresholding rule.

Figure 9. Comparative performance of Table 1 methods on standard images with noise level 30

TABLE 5. Comparative PSNR results of proposed method and recent denoising works

	Lena		Barbara		peppers	
σ	20	30	20	30	20	30
[36]	30.77	29.04	28.55	27.38	30.57	28.83
[37]	30.92	29.13	28.48	26.27	30.57	28.83
[38]	28.25	25.7	26.81	24.49	26.96	25.03
[39]	31.16	29.25	28.71	26.59	30.81	28.92
our work	**31.21**	**29.44**	**30.08**	**28.82**	**31.07**	**29.36**

The SURELET method produces a similar result on edges. However, as can be perceived through Figure 9, The proposed method outperforms SURELET in homogeneous regions, producing smoother results. That can be clearly observed in the various homogeneous regions in the images. The GIF, FBF, Bivariate and Bayes methods fail to smooth images when noise increases to higher levels. These produce good results at lower σ values but give poor denoised images at higher noise levels. The TV method tends to oversmooth the image. Due to this reason some fine structures of the original image are not being preserved in the filtered output image.

5. CONCLUSION

In this paper, an efficient noise removal framework based on curvelet transform and Wiener filter was presented. With utilizing wavelet fusion, the denoised image had few line artifacts (disadvantage of curvelet denoising) and was less blurred (disadvantage of wiener filter). Two criteria, PSNR and SSIM were selected to evaluate the performance of proposed method. The obtained results indicated that our method could remove the noise better than the curvelet transform and wiener filter alone. It was shown that Denoising by curvelet transform improved %6.3 in terms of PSNR and %5.9 in terms of SSIM for 'Lena' image. Furthermore, the proposed framework was compared with recent reported method and it indicated superiority of the introduced framework.

6. REFERENCES

1. Khosravi, M. and Hassanpour, H., "Image denoising using anisotropic diffusion equations on reflection and illumination components of image," *International Journal of Engineering-Transactions C: Aspects*, Vol. 27, No. 9, (2014), 1339-1348.

2. Nadernejad, E., Hassanpour, H. and Miar, H., "Image restoration using a pde-based approach," *International Journal of Engineering Transactions B: Applications*, Vol. 20, No. 3, (2007), 225-236.

3. Keyvanpour, M., Tavoli, R. and Mozafari, S., "Document image retrieval based on keyword spotting using relevance feedback", *International Journal of Engineering-Transactions A: Basics*, Vol. 27, No. 1, (2013), 7-14.

4. Farbiz, F., Menhaj, M. and Motamedi, S., "A new iterative fuzzy-based method for image enhancement", *International Journal of Engineering*, Vol. 13, No. 3, (2000), 69-74.

5. Hassanpour, H. and Ghadi, A. R., "Image enhancement via reducing impairment effects on image components", *International Journal of Engineering-Transactions B: Applications*, Vol. 26, No. 11, (2013), 1267-1274.

6. Candes, E. J. and Donoho, D. L., "Curvelets: A surprisingly effective nonadaptive representation for objects with edges", DTIC Document, (1999).

7. Candes, E. J. and Donoho, D. L., " Continuous curvelet transform I: Resolution of the Wavefront Set ", *Applied and Computational Harmonic Analysis*, Vol. 19, No. 2, (2005), 162-197.

8. Candes, E. J. and Donoho, D. L., "Continuous curvelet transform: II. Discretization and frames", *Applied and Computational Harmonic Analysis*, Vol. 19, No. 2, (2005), 198-222.

9. Stehly, L., Cupillard, P. and Romanowicz, B., "Towards improving ambient noise tomography using simultaneously curvelet denoising filters and SEM simulations of seismic ambient noise", *Comptes Rendus Geoscience*, Vol. 343, No. 8, (2011), 591-599.

10. Palakkal, S. and Prabhu, K., "Poisson image denoising using fast discrete curvelet transform and wave atom", *Signal Processing*, Vol. 92, No. 9, (2012), 2002-2017.

11. Bhadauria, H. and Dewal, M., "Medical image denoising using adaptive fusion of curvelet transform and total variation," *Computers & Electrical Engineering*, Vol. 39, No. 5, (2013), 1451-1460.

12. Lin, F. and Jin, C., "An improved wiener deconvolution filter for high-resolution electron microscopy images," *Micron*, Vol. 50, (2013), 1-6.

13. Mohan, J., Krishnaveni, V. and Guo, Y., "MRI denoising using nonlocal neutrosophic set approach of wiener filtering", *Biomedical Signal Processing and Control*, Vol. 8, No. 6, (2013), 779-791.

14. Zhang, X., Feng, X., Wang, W., Zhang, S. and Dong, Q., "Gradient-based wiener filter for image denoising", *Computers & Electrical Engineering*, Vol. 39, No. 3, (2013), 934-944.

15. Gonzalez, W. and Woods, R. E., "Eddins, digital image processing using matlab", *Third New Jersey: Prentice Hall*, (2004).

16. Lim, J. S., Two-dimensional signal and image processing, *Englewood Cliffs, NJ, Prentice Hall,* Vol. 1, (1990).

17. Shensa, M. J., "The discrete wavelet transform: Wedding the a trous and mallat algorithms", *IEEE Transactions on signal processing*, Vol. 40, No. 10, (1992), 2464-2482.

18. Andrew, B. and Hongye, G., "Wave shrinkage function and thresholds", in SPIE. Vol. 2569, (1995), 270-281.

19. Donoho, D. L. and Johnstone, J. M., "Ideal spatial adaptation by wavelet shrinkage", *Biometrika*, Vol. 81, No. 3, (1994), 425-455.

20. Cai, T. T. and Silverman, B. W., "Incorporating information on neighbouring coefficients into wavelet estimation", *Sankhya: The Indian Journal of Statistics, Series B*, (2001), 127-148.

21. Haghighat, M. B. A., Aghagolzadeh, A. and Seyedarabi, H., "Multi-focus image fusion for visual sensor networks in DCT domain", *Computers & Electrical Engineering*, Vol. 37, No. 5, (2011), 789-797.

22. Haghighat, M. B. A., Aghagolzadeh, A. and Seyedarabi, H., "A non-reference image fusion metric based on mutual information of image features", *Computers & Electrical Engineering*, Vol. 37, No. 5, (2011), 744-756.

23. Zeeuw, P. M., "Wavelet and image fusion", *CWI, Amsterdam*, (1998).

24. Wang, Z., Bovik, A. C., Sheikh, H. R. and Simoncelli, E. P., "Image quality assessment: From error visibility to structural similarity", *IEEE Transactions on Image Processing*, Vol. 13, No. 4, (2004), 600-612.

25. Wang, Z. and Bovik, A. C., "A universal image quality index", *IEEE Signal Processing Letters*, Vol. 9, No. 3, (2002), 81-84.

26. Blu, T. and Luisier, F., "The sure-let approach to image denoising", *IEEE Transactions on Image Processing*, Vol. 16, No. 11, (2007), 2778-2786.

27. Sendur, L. and Selesnick, I. W., "Bivariate shrinkage with local variance estimation", *IEEE Signal Processing Letters*, Vol. 9, No. 12, (2002), 438-441.

28. Chang, S. G., Yu, B. and Vetterli, M., "Adaptive wavelet thresholding for image denoising and compression", *IEEE Transactions on Image Processing*, Vol. 9, No. 9, (2000), 1532-1546.

29. Qiu, T., Wang, A., Yu, N. and Song, A., "Llsure: Local linear sure-based edge-preserving image filtering", *IEEE Transactions on Image Processing*, Vol. 22, No. 1, (2013), 80-90.

30. He, K., Sun, J. and Tang, X., "Guided image filtering", in European conference on computer vision, Springer, (2010), 1-14.

31. Yang, Q., Tan, K.-H. and Ahuja, N., "Real-time o (1) bilateral filtering", 2009 IEEE Conference on Computer Vision and Pattern Recognition, (2009), 557-564.

32. Rudin, L. I., Osher, S. and Fatemi, E., "Nonlinear total variation based noise removal algorithms", *Physica D: Nonlinear Phenomena*, Vol. 60, No. 1, (1992), 259-268.

33. Pratt, W., Digital Image Processing, New York: Wiley, (1978).

34. Crete-Roffet, F., Dolmiere, T., Ladret, P. and Nicolas, M., "The blur effect: Perception and estimation with a new no-reference perceptual blur metric", in SPIE Electronic Imaging Symposium Conf Human Vision and Electronic Imaging. Vol. 12, (2007), 6492-6416.

35. Qu, X., Hu, C. and Yan, J., "Image fusion algorithm based on orientation information motivated pulse coupled neural networks", 2008 7th World Congress on Intelligent Control and Automation, (2008), 2437-2441.

36. Om, H. and Biswas, M., "A generalized image denoising method using neighbouring wavelet coefficients", *Signal, Image and Video Processing*, Vol. 9, No. 1, (2015), 191-200.

37. Om, H. and Biswas, M., "Mmse based map estimation for image denoising", *Optics & Laser Technology*, Vol. 57, (2014), 252-264.

38. Jain, P. and Tyagi, V., "An adaptive edge-preserving image denoising technique using tetrolet transforms", *The Visual Computer*, Vol. 31, No. 5, (2015), 657-674.

39. Biswas, M. and Om, H., "A new adaptive image denoising method based on neighboring coefficients", *Journal of The Institution of Engineers (India): Series B*, Vol. 97, No. 1, (2016), 11-19.

An Efficient Curvelet Framework for Denoising Images

E. Ehsaeyan

Department of Electrical and Electronics Engineering, Sirjan University of Technology

چکیده

فیلتر وینر می تواند نویز تصاویر را بصورت موثری حذف نماید. اما استفاده از فیلتر وینر باعث تار شدن تصویر خروجی می شود. تبدیل کرولت قابلیت حفظ لبه ها را در تصاویر طبیعی دارد. ولی به تصویر خروجی، اثرات مصنوعی و لبه های مجازی اضافه می کند. بخصوص در مناطق همگن تصویر. در این مقاله، یک طرحواره حذف نویز تصاویر برپایه تبدیل کرولت و فیلتر وینر پیشنهاد شده است که قابلیت بهتری برای کم کردن اثر نویز در خروجی، در مقایسه با روش های ذکر شده دارد. کارایی روش پیشنهادی توسط دو معیار مهم رفع نویز، یعنی نسبت سیگنال به نویز و ضریب تشابه، برای تصاویر نمونه در سطوح مختلف نویزی، مورد ارزیابی قرار گرفته است. سه آستانه گیری معروف یعنی 'ملایم' ، 'نیمه ملایم' و 'سخت' بر تصاویر نویز دار اعمال می شود و نتایج توسط تبدیل ویولت، به هم پیوند می خورند. ساختار پیشنهادی، رفع نویز بوسیله تبدیل کرولت را به اندازه ٦.٣٪ از لحاظ PSNR و ٥.٩٪ از لحاظ SSIM برای تصویر Lena ، بهبود می بخشد. تصاویر خروجی حاکی از آن است که اثرات پارازیتی و درجه تارشدگی تصاویر خروجی، بطور قابل ملاحظه ای کاهش می یابد. نتایج بدست آمده نشان می دهد که عملکرد طرحواره پیشنهادی، از روش های گزارش شده اخیر، بالاتر می باشد.

doi: *10.5829/idosi.ije.2016.29.08b.09*